Integration of a Combined Heat, Hydrogen and Power System at Sines Refinery Power Plant using Solid Oxide Fuel Cells

Catarina Mendonça

Abstract

The feasibility of a Combined Heat, Hydrogen and Power (CHHP) system to implement at Galp's refinery is studied, using Solid Oxide Fuel Cells (SOFC) as a clean power source. To evaluate its feasibility, this trigeneration system was simulated using Aspen Plus V11 software. Considering 10 kmol/h of fuel gas and 219.8 kmol/h of fresh air, 16.5 kg/h of hydrogen (99.999% purity) and 3 MMBtu/hr of heat were produced. Regarding the electrical power produced, it was determined by modelling the SOFC using the partial pressures of hydrogen, oxygen and water from Aspen Plus as input data and the result was 1.06 MW. Additionally, an economic analysis was included on this study to understand if the investment carried out would be viable. From this point of view, the production of high purity hydrogen presents a more significant impact on the profitibility of the trigeneration system than the electrical energy production, since the generated profit can compensate the investment performed on a 3 to 4 years period.

Keywords

Trigeneration; Solid Oxide Fuel Cell; High-Purity Hydrogen; Clean Power

Contents

1. Introduction

It is crucial to develop advanced clean energy systems in order to switch from a fossil fuel-based economy to a new paradigm structure [1]. The hydrogen economy has been proposed as a possible method in which hydrogen plays as one of the main global energy carriers. It can be applied in fuel cells to generate power from an electrochemical reaction rather than combustion, producing only water and heat as byproducts, providing energy for transportation, buildings, and industry [2].

Fuel cell technologies are achieving a lot of attention through research and industry sectors due to their potential to provide long-term durability clean energy to consumers, high energy conversion efficiencies, flexibility in design, and flexibility in fuel choice [3]. Additionally, they possess a static nature that reflects on a silent operation, while their implicit modularity grants for simple construction and adverse range of applications in portable, stationary, and transportation power generation [4]. Each cell is composed of four main parts: anode, cathode, electrolyte, and the external circuit. There are multiple designs available for fuel cells yet, they all operate according to the same assumptions, the only difference is the chemical characteristics of the electrolyte [5].

Regarding the several types of fuel cells, these types include proton exchange membrane fuel cells (PEMFCs), direct methanol fuel cells (DMFCs), alkaline fuel cells (AFCs), molten carbonate fuel cells (MCFCs), phosphoric acid fuel cells (PAFCs) and solid oxide fuel cells (SOFCs) [6].

One of the multiple applications fuel cells is their incorporation in the trigeneration concept - Combined Hydrogen, Heat and Power (CHHP). The most suitable candidates to be applied in CHHP are High-Temperature Fuel Cells (HTFCs), MCFCs and SOFCs, which release enough heat during electrochemical reactions to efficiently produce hydrogen in order to be separated and purified for transportation purposes for instance. Both systems are among the HTFCs that present higher electrical efficiency and lower CO_2 emissions when in comparison with fossil fuel power plants [7]. Regarding stationary power plant applications, SOFC is the dominant technology since it has a relatively higher power density and is

less corrosive than the MCFC, which due to the nature of the electrolyte (molten salt), can be lost throughout a long term operation. In SOFCs, hydrocarbon fuels are reformed internally, generating a mixture of hydrogen and carbon monoxide, while air is used as the oxidant in the fuel cell [8]. Yttria stabilized zirconia (YSZ) is the most frequently used electrolyte for this type of fuel cell due to its high chemical and thermal stability and pure ionic conductivity [9, 10]. Oxygen is reduced at the cathode, while fuel oxidation occurs at the anode (1,2 and 3). A porous anode facilitates fuel conduction and transportation of products away from the electrolyte and fuel electrode interfaces [11, 12].

Anode:

$$H_2 + O^{2-} \rightarrow H_2O + 2e^- \tag{1}$$

$$CO + O^{2-} \rightarrow CO_2 + 2e^- \tag{2}$$

Cathode:

$$O_2 + 4e^- \rightarrow 2O^{2-} \tag{3}$$

Additionally, SOFCs integrated in stationary power plants are capable of producing useful power (electricity and heat) and hydrogen with a high efficiency associated. This can come as a solution for industries to achieve greater productivity and quality in their products and still manage to engage a more rational and sustainable use of primary energy resources.

In Portugal, there is a tight policy regarding CO_2 emissions, taxes are increasing exponentially, and incentives to search for greener technologies are becoming more predominant [13]. Galp is responsible for the largest hydrogen production and utilization in Portugal. Recently, it has joined the Hydrogen Council, an association of large companies and institutions worldwide that aspires to promote the development of hydrogen as the most competitive solution for the decarbonization of many sectors of the economy. Galp's large-scale projects are mainly directed to the production of green hydrogen from renewable energy and its association with the decarbonization of industrial processes and mobility or for injection into natural gas networks. These projects are included in the company's strategic objective of directing approximately 40% of its net annual investment to opportunities related to the energy transition, and that contribute to globally reduce CO_2 emissions [14]. In this manner, Trigeneration systems may be a huge opportunity to reduce not only primary energy consumption but also achieve economic benefits, increase electrical reliability, and produce a new feed of high purity hydrogen for different purposes.

Regarding Galp's refinery, its located in Sines, comprises four plants. Plants I, II, and III are responsible for producing Liquified Pretoleum Gas (LPG), naphtha, gasoline, middle distillates, and fuel. Utilities demanded by these, such as steam, electrical energy, demineralized water, cooling water, fuel oil, among others, are produced in the fourth plant which is known as *Utilidades*. Herein, a Cogeneration system was implemented in 2009, comprising two recovery boilers equipped with an afterburner system (Heat Recovery Steam Generator - HRSG) and two Gas Turbines (GTs) to produce High Pressure (HP) steam and electrical energy, respectively, by burning natural gas [15].

Overall, the electrical energy generated corresponds to 82 MWh (2×41 MWh) which is sell in the wholesale market with a Feed In Tariff. Electrical demand of Sines Refinery is supplied by conventional steam turbines and the remained consumption feed by an interconnection with Portuguese Trasmission System Operator (TSO), *Rede Elétrica Nacional* (REN). Nevertheless, for the GT's start-up, it is required an electrical energy consumption from the auxiliary equipment, which, afterward, is no longer needed since it begins to be auto consumed, meaning part of the energy produced is used to supply that equipment. Moreover, approximately 50% of the utility produced is injected into the Portuguese TSO (REN).

Therefore, studying the possibility of providing electrical energy for GTs auxiliary equipment could substantially improve the cogeneration system's efficiency since a more significant amount of electrical energy would be injected into REN, bringing economic benefits.

This thesis intends to evaluate the techno-economic feasibility of implementing a CHHP system integrated with a SOFC system fuelled with fuel gas. The main objectives are to attain an electrical power output of around 1.06 MW for GTs auxiliary equipment and produce hydrogen to supply refueling stations. In addition, reduce a considerable amount of CO_2 emissions with the SOFC system and the exploitation of the fuel gas, avoiding discharges on the flare.

2. Aspen Implementation

2.1 Assumptions for Process Simulation

The feasibility of a CHHP system was tested in the process simulation software widely known as Aspen Plus V11. The model developed by Bloom Energy, Server ES5-250 kW, was the one chosen for the SOFC system, due to the availability of the information and since it is one of the most mature technologies in the market. This server is built up with 1 kW electricity stacks, labeled as 'Bloom Boxes', which are composed of 40 cells of 25 W electricity each, operating at 850ºC [16, 17]. The output voltage of each cell is 0.8V DC [18]. According to Bloom's patent description, the electrolyte corresponds to Scandia stabilized Zirconia (ScSZ). The anode and cathode are made from special inks that coat the electrolyte. The anode side is coated with a green nickel oxide-based ink, and the cathode side is coated with black ink (Lanthanum Strontium Manganite) [19].

Regarding choosing the proper thermodynamic model for this simulating, in oil, gas, and petrochemical applications, the Peng-Robison property package is commonly recommended [20].

The following assumptions are made in this simulation process [21]: (i) steady-state; (ii) ideal gas model; (iii) reactions are in a chemical equilibrium condition;(iv) the pressure drop

in all equipment is ignored; (v) only H_2 is involved in the electrochemical reaction in the anode (vi) the values of consumed H_2 in the electrochemical reaction is considered as the input of the model; (vii) the amount of consumed O_2 in the electrochemical reaction is considered to be a known input; (viii) pure oxygen is provided in the cathode.

2.2 Input Auxiliary Calculations

The fuel provided by Galp's Refinery corresponds to fuel gas with the composition presented in Table 1. This fuel gas will be submitted to a steam reforming process inside the fuel cell, producing hydrogen required for the electrochemical reaction.

Table 1. Molar composition of the fuel gas provided by Galp, Sines Refinery.

Component	Composition (mol. %)
H_2	40.8
CH_4	33.4
C_2H_6	12.8
C_3H_8	13.0

These values were obtained through chromatography and represented an average of the fuel gas composition between January and April of 2021. Propane concentration also takes into account C_4+ since their concentrations are almost negligible compared to the other components, and it simplifies the following calculations.

Considering an 88% efficiency in the AC/DC converter, to obtain 1.06 MW of AC power, 1.2 MW should be produced by the fuel cell. Additionally, it was assumed a voltage of 0.8 V and a U_f of 85%. With these values a fuel gas flow of 8.38 kmol/h and dry air flow of 222.7 kmol/h was initially determined.

2.3 Process Description

Figure 1 represents the flowsheet simulated in Aspen PLus V11 for the Combined Heat, Hydrogen and Power system. Aspen Implementation

2.3.1 Pre-Reforming

Fuel gas enters the CHHP system at atmospheric pressure suffering a slight increase by "COMP1". Part of the anode exhaust is recycled "RECIRC1" (33%) to help to reach an H_2O-to-CH_4 ratio of 2.5–3.0, which is of standard practice in industry [22]. Nevertheless, fresh water, WATERIN, is also required to maintain this ratio. The feedstock is cleaned of contaminants that could degrade the system, such as sulfur (from the fuel) and salts (from the water). The resulting mixture will be submitted to a partial reforming (block "REFORM"). The chosen reactor was RStoic, operating at 700 ºC. This reactor simulates precisely the reforming reactions specified below, and it considers as input the intention of converting 20% of the existing hydrocarbons [22].

2.3.2 Anode

Before entering the anode compartment, the resulting gas (REF-OUT) passes through an electric heat exchanger, HX3, to increase the temperature to 850 ºC, which corresponds to the working temperature of the SOFC chosen in this study [17]. In the ANODE block, the remaining hydrocarbons are reformed, CO is shifted. Stream "O2" delivers pure O_2 for H_2 oxidation. The "ANODE" block is characterized by the equilibrium reactor module RGibbs working in isothermal conditions.

2.3.3 Cathode

Preheated air enters the cathode, modeled as a separator block ("CATHODE") which simulates the mass transfer of oxygen ions required for the electrochemical reaction 3 [21]. Using this model, the amount of oxygen that is separated from the air and reacts with H_2 can be defined based on split fraction. This parameter was considered to be 0.3.

2.3.4 Heat Integration

Reactions in block "REFORMER" are endothermic. Thus part of the anode exhaust gas ("PRE-HX2") is used to preheat the steam and fuel mixture up to a reasonable temperature for the catalytic reactor in block "HX2". Afterward, the remaining gas mixture that was not recycled back to the system, stream "ANODE3", serves as a hot utility in block "HX4" for the air preheating process. Finally, the outlet stream depleted from O_2 ("AIR-OUT") is also used for heat integration owing to its elevated temperature. It is responsible for the heat transfer in block "HX5".

2.3.5 Water Gas Shift (WGS)

Stream "ANODE 4" goes through a shift reaction and is diverted for purification and storage of hydrogen. Therefore, it is cooled down to 300 ºC, which is favorable for the WGS reaction. REquil ("WGS") was the block chosen to simulate this reaction considering "Temperature Approach" as specification type.

2.3.6 Pressure Swing Adsorption

The optimum feed pressure to the PSA ranges from 15 to 29 bar [5]; the inlet pressure for this model is chosen to be 18 bar. A multi-stage compressor represented by "COMP4" to "COMP7" is used with a maximum compression ratio of 2:1 per stage and intercoolers to 25°C. In the Aspen model, water is removed after each compression stage [22]. The PSA unit is modeled as a separator block. The composition requirement for hydrogen at the inlet of the PSA unit is 70% thus, in order to achieve it 88 % of the purified hydrogen is recycled to the PSA inlet, represented by the stream "H2-2". [23]. The "TAILGAS" stream will be depressurized and used for heating applications.

3. Results and Discussion

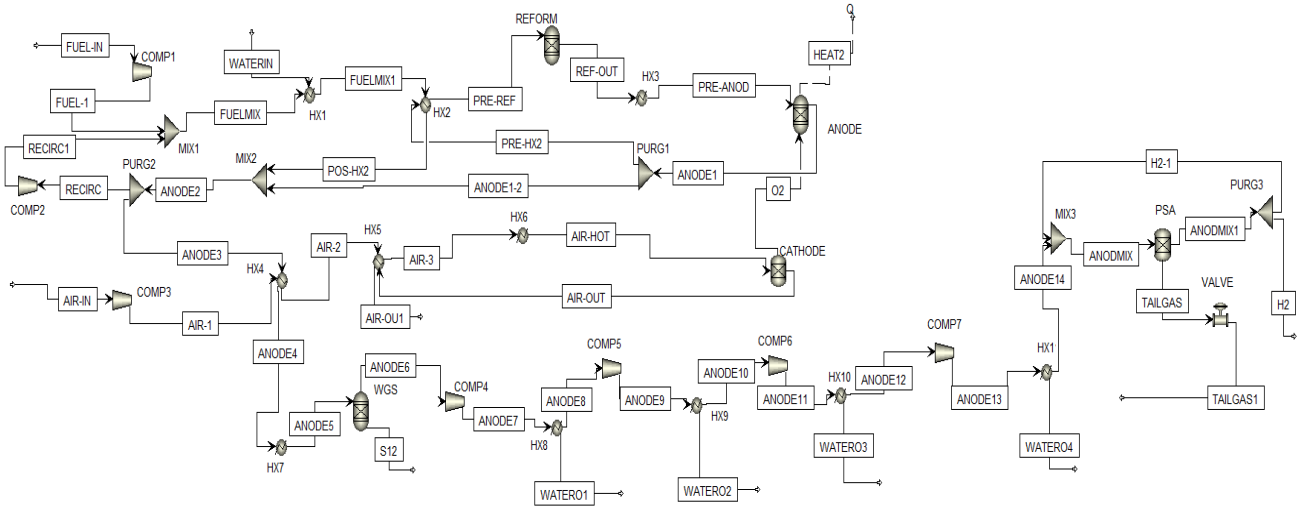

Figure 1. Flowsheet of CHHP Process simulation.

3.1 SOFC Modelling

SOFC modeling has as main objective to generate the expected stack performance and express its sensitivity to temperature, pressure, and compositional variations in the reactant feed gases. Aspen Plus software does not allow determining the cell's voltage and, consequently, power production, which are crucial parameters to validate the implemented system and preliminary calculations. Two different approaches were used to determine the cell voltage.

3.1.1 Approach 1

The method used in the proposed model combines a performance curve obtained by interpolation of experimental data at standard operating conditions, as a reference. Afterward, it predicts the cell voltage by applying semi-empirical correlations [24, 25]. The current model adopts a reported experimental curve [24] as the reference curve to define the reference voltage V_{ref} at the referenced operating condition (inlet fuel composition: 67% H_2, 22% CO, 11% H_2O, 85% U_f, T=1000 ºC and P=1 bar). Regarding the semi-empirical equations, the operating pressure is defined by Eq. 4 [24, 25]:

$$\Delta V_{\mathrm{p}}(mV) = 76 \times log\frac{P}{P_{\mathrm{ref}}} \tag{4}$$

where P is the operating pressure (bar) and P_{ref} is the reference operating pressure (here P_{ref}=1 bar).

The operating temperature and the current density are related by the expression shown in Eq.5:

$$\Delta V_{\mathrm{T}}(mV) = 0.008 \times (T - T_{\mathrm{ref}})(C) \times I_{\mathrm{c}}(mA/cm^2) \tag{5}$$

where T is the operating temperature and T_{ref} is the reference operating temperature (here T_{ref}=1000 ºC). The current density defined as I_c was considered 80 A/cm^2.

Lastly, the fuel and oxidant compositon are determined by Eq. 6 and 7:

$$\Delta V_{\mathrm{anode}}(mV) = 172 \times log\frac{P_{\mathrm{H_2}}/P_{\mathrm{H_2O}}}{(P_{\mathrm{H_2}}/P_{\mathrm{H_2O}})_{\mathrm{ref}}} \tag{6}$$

where P_{H_2}=P_{H_2O} is the ratio of H_2 and steam partial pressures in the system and $(P_{H_2}/P_{H_2O})_{ref}$ is the ratio of H_2 and steam partial pressures in the system under reference conditions (here $(P_{H_2}/P_{H_2O})_{ref}$=0.15).

$$\Delta V_{\mathrm{cathode}}(mV) = 92 \times log\frac{P_{\mathrm{O_2}}}{(P_{\mathrm{O_2}})_{\mathrm{ref}}} \tag{7}$$

where P_{O_2} and $(P_{O_2})_{ref}$ are the average oxygen partial pressures at the cathode for the actual case and the reference case, respectively ($(P_{O_2})_{ref}$=0.164).

Note that in the ΔV_{anode} and $\Delta V_{cathode}$, the values of P_{H_2}, P_{H_2O} and P_{O_2} correspond to an average between the inlet and outlet of the fuel cell [26]. By summing the four correlations, the actual voltage V can be calculated as in Eq. 8:

$$V = V_{\mathrm{ref}} + \Delta V_{\mathrm{T}} + \Delta V_{\mathrm{P}} + \Delta V_{\mathrm{anode}} + \Delta V_{\mathrm{cathode}} \tag{8}$$

The fuel cell power output is the product of the cell voltage and current. The developed model takes the desired power output as an input to calculate the corresponding voltage and current required to generate the power. Then, if the product between these parameters does not match the desired power output, the amount of fresh fuel is corrected according to the hierarchy of the calculations.

3.1.2 Approach 2

On this approach, the cell voltage is determined through equation 9 [27]. Herein, the fuel cell operating conditions were also modeled based on the inlet and outlet's average temperature and fuel composition. The nominal operating temperature

of the stack is estimated to be 850 ºC with a per-pass fuel utilization of 85%.

$$V = OCV_{\text{Nernst}} - \eta_{\text{act}} - \eta_{\text{ohm}} - \eta_{\text{conc}} \quad (9)$$

where $\text{OCV}_{\text{Nernst}}$ is the open circuit voltage, and the η terms are the activation, ohmic, and concentration losses described below. The $\text{OCV}_{\text{Nernst}}$ accounts for temperature and composition dependence of the Nernst voltage, as well as the deviation of the experimental OCV voltage from theory in agreement with 10:

$$OCV_{\text{exp}} = E_0 + \frac{RT}{nF} ln\Big[\frac{P_{H_2} {P_{O_2}}^{0.5}}{P_{H_2O}} {P_{\text{atm}}}^{0.5}\Big] \quad (10)$$

where from [25]

$$E_0 = 1.2723 - 2.7645 \times 10^{-4} \times T \quad (11)$$

and n = 2 and F = 96 485 C/mol. Deviation of the experimental OCV from the Nernst voltage is accounted in:

$$\theta = \frac{OCV_{\text{exp}}}{OCV_{\text{Nernst}}} \quad (12)$$

where θ refers to the electronic and ionic conductivity of the electrolyte in open circuit conditions [28]. This factor is approximately 0.94 [28]. The activation polarization, η_{act}, is inherently calculated from the Butler–Volmer equation 13:

$$j = j_0\Big[exp\Big(\alpha\frac{nF}{RT}\eta_{\text{act}}\Big) - exp\Big(-(1-\alpha)\frac{nF}{RT}\eta_{\text{act}}\Big)\Big] \quad (13)$$

where α is the charge transfer coefficient, and j_0 corresponds to a pre-exponential factor specific to each electrode expressed by 14 and 15:

$$j_{0,\text{c}} = \gamma_{\text{c}}\Big(\frac{P_{O_2}}{P_{\text{atm}}}\Big)^{0.25} exp\Big(-\frac{E_{\text{act,c}}}{RT}\Big) \quad (14)$$

$$j_{0,\text{a}} = \gamma_{\text{a}}\Big(\frac{P_{H_2}}{P_{\text{atm}}}\Big)\Big(\frac{P_{H_2O}}{P_{\text{atm}}}\Big) exp\Big(-\frac{E_{\text{act,a}}}{RT}\Big) \quad (15)$$

where γ is an activation over-potential factor and E_{act} is the activation energy; these values are obtained from [29]. The charge transfer coefficient, α, typically ranges from 0.2 to 0.5 [30]. Furthermore, in reversible reactions (an usual assumption made for SOFC kinetic behaviour), the chemical and electrical energy form equal activation barriers for the forward and reverse reactions, thus α= 0.5 [30]. This simplification is used to reduce Eq. 13 to 16:

$$j = 2j_0 sinh\Big(\frac{nF}{2RT}\eta_{\text{act}}\Big) \quad (16)$$

The ohmic loss term, η_{ohm}, is dependent on both the resistivity of the stack components, and their thicknesses as demonstrated in Eq. 17:

$$\eta_{\text{ohm}} = j \times ASR_{\text{ohm}} \quad (17)$$

where ASR_{ohm} is the ohmic area specific resistance estimated from [29] to be 0.04 Ω cm^2. The concentration losses, η_{conc}, are obtained by the limiting current density in the subsequent Eq.18:

$$\eta_{\text{conc}} = \frac{RT}{nF} ln\Big(1 - \frac{j}{j_{\text{L}}}\Big) \quad (18)$$

where j_{L} is the limiting current density and is predicted to be 1.6 A/cm^2 at 800 ºC from [31].

3.2 Modelling Results

The fuel flow and, consequently, oxidant flow were adjusted until the desired power output was reached. It should be mentioned that for every attempt, the water flow is also correct in order to respect the S/C ratio.

Table 2. Final Results of SOFC Modelling for the CHHP system developed in Aspen Plus V11.

	Approach 1	Approach 2	Units
n_{fuel}	8.27		kmol/h
n_{air}	219.8		kmol/h
$n_{\text{fresh water}}$	4.6		kmol/h
I	1 485		kA
ΔV	0.873	0.812	V
P_{DC}	1.296	1.206	MW
P_{AC}	1.140	1.060	MW

Table 2 indicates that Approach 2 determines a cell voltage quite accurately with the one considered by Bloom Energy (0.8 V) besides reaching the desired output power. Contrarily, Approach 1 presents a higher cell voltage and, therefore, a higher output power (AC), with a relative error of 52%.
It is possible to conclude that Approach 2 is more accurate than Approach 1, which was already expected since it takes into account activation, ohmic polarization, and concentration losses with a temperate and pressure dependency (see equations 16, 17). Additionally, it is the SOFC model generally used in the research community. Whilst Approach 1, even though it is a reliable method to apply, considers semi-empirical equations that account only for the effects of operating pressure and temperature, current density, and fuel/air composition on the actual voltage. However, the voltage losses in SOFCs are governed by ohmic losses in the cell components, which are not directly accounted in this Approach and may be a valid reason for the difference observed [24]. Thus, in the following subjects, Approach 2 was the one considered to determine the SOFC parameters.

3.2.1 Hydrogen and Heat Production

Hydrogen and Heat production are also crucial parameters to be examined in this study. Using the results obtained in Table 2 and implementing the specifications stated in **subsubsection 2.3.6**, H_2 flow is 3.9 kg/h corresponding to a daily production of 95 kg/day (31.4 ton/year). Regarding the heat produced,

stream TAILGAS1, with an enthalpy of 3.02 MMBtu/h, could be used for a building heating system or a water cycle, entering at 60°C and being heated to 80°C before returning to the facility. Nevertheless, this part was not simulated in Aspen Plus in order to simplify the system developed and since the amount of heat produced is almost negligible. Since there is an additional interest in hydrogen over-production and considering that the value obtained is quite inferior in comparison to the three methods for hydrogen production presented in Table 3, fuel cell utilization was decreased by maintaining the same amount of oxidant entering the cathode but increasing the amount of fuel entering the anode.

Table 3. Comparison between the amount of hydrogen produced from different processes [105].

Process	H_2 Production	Units
SMR of Natural Gas (large-scale)	150 000	kg/day
SMR of Natural Gas (distributed-scale)	250	kg/day
Electrolysis	1 050	kg/day

Table 4. Results for hydrogen over-production in CHHP implemented on Aspen Plus.

Parameter	Value	Units
n_{fuel}	10	kmol/h
n_{air}	219.8	kmol/h
$n_{fresh\ water}$	6.50	kmol/h
ΔV	0.817	V
I	1 485	kA
P_{DC}	1.213	MW
P_{AC}	1.067	MW
H_2 production	16.5	kg/h
H_2 production	396	kg/day
H_2 production	130 680	kg/year

Results demonstrate a considerable increase in hydrogen production with the change from 8.27 kmol/h to 10 kmol/h of fuel. The SOFC operating voltage increases slightly (5 mV) due to a higher content of reactant hydrogen (which increases the Nernst potential) and a reduction in fuel utilization. Nevertheless, as it was expected, the power output remains approximately equal. The desired value of hydrogen production will only be possible to examine with the Economic Analysis of the system implemented.

3.2.2 Sensitivity Analysis

Aspen Plus software provides the possibility to perform sensitivity analysis, which simplifies understanding the effects of variations of the operating parameters on the SOFC's performance. The utilization factor is one of the most important operating parameters for fuel cells and has significant effects on the cell voltage and current intensity [24]. Figures 2 and 3 depict the influence of U_f on SOFC stack performance, for both cell voltage and current intensity.

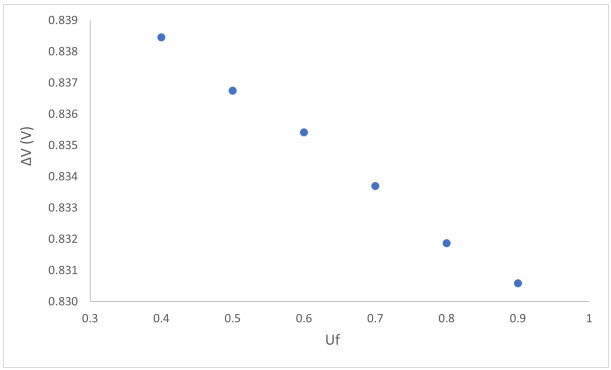

Figure 2. Effects of U_f on the cell voltage.

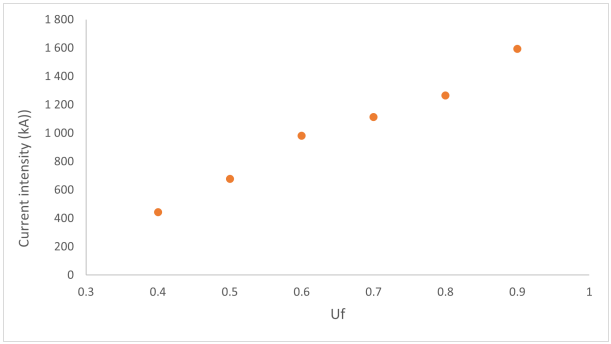

Figure 3. Effects of U_f on the current.

Increasing U_f from 0.4 to 0.9, implies a decrease in the cell voltage since the fuel is more depleted and the voltage losses at the anode are increased. In contrast, the current intensity will increase, which can be accomplished by increasing the airflow, resulting in more H_2 being consumed in the anode ($I = 2FnH_2$,consumed) [25, 32]. Therefore, operating the SOFC stack at high fuel utilization promotes a higher current intensity and, consequently, higher power output. However, it should be analyzed if the voltage losses aren't increasing substantially. Usually, 0.85 for the U_f is considered [26, 32]. Besides evaluating the SOFC performance for power production, hydrogen production was also submitted to sensitive analysis at different values of U_f represented in Fig. 4.

A higher amount of fuel gas input is reformed and, with a constant U_f, the hydrogen not consumed by the fuel cell increases in the same proportion that hydrogen is converted in the electrochemical reaction. Moreover, decreasing the U_f leads to an increase in hydrogen production, which was already expected since less hydrogen is consumed by the SOFC, being available for the recovery process. Lastly, values between 600 and 1 200 kg/day are possible to reach, which is comparable to the amounts claimed to be produced in Table 3, therefore justifying the possible feasibility of this project.

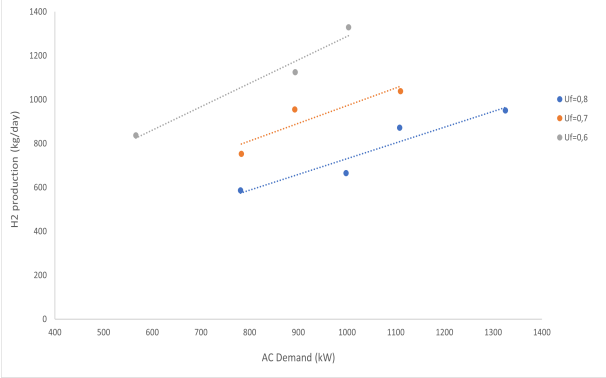

Figure 4. Effects of AC demand on the Hydrogen Production.

4. Economic Analysis

An economic analysis of the studied system is crucial to determine whether it is worth the investment carried out. Thus, it was considered a 3 years duration for the project investment and construction and 20 years for the exploration period.
According to [33] SOFCs should be replaced every five years. In order to obtained more detailed information Bloom Energy was contacted, however, no response was received and thus we have assumed the worst case scenario which considers an acquisition of new servers every five years [33].
The total investment of this CHHP system was determined, as well as operation costs. Lastly, taking these into account and the generated profit regarding the generation of electrical energy and hydrogen production, it was possible to evaluate the economic benefits of the project. The payback time (time the project takes to recover the invested capital) is also determined [34]).

4.1 Total Investment

This project will only focus on determining the fixed capital investment which is divided into two main groups: direct costs and indirect costs [35]. Regarding direct costs, these include equipment base costs which will be analysed in further detail. Equipment costs were estimated using the cost scaling equation given in Eq. 19. The cost of each scaling unit (S) is established using the reference scaling unit (S_0) and its base cost (C_0). The superscript n corresponds to the scaling factor, which considers the economy of scale of a particular component. Using the Chemical Engineering Plant Cost Index (CEPCI), the cost is updated following the changes in the value of money due to inflation and deflation and (I_F) is the installation factor which takes into account the multiple costs associated with installing each equipment [27].

$$IC = \left(\frac{S}{S_0}\right)^n \left(\frac{CEPCI}{CEPC_0}\right) I_F \tag{19}$$

The equipment and installation costs are included in the direct costs (DC). These also consider utilities, services, piping, instrumentation, control, buildings, electrical installation, and thermal isolation costs. To estimate these, a percentage on the equipment base cost was considered, as demonstrated in Table 5 [35].

Table 5. Direct costs for the CHHP system.

	Cost (M€)	Factor (%BE)
Base Equiment (BE)	5.808	-
Piping	1.452	0.25
Services and Utilities	0.580	0.10
Control and Instrumentation	0.290	0.05
Buildings	0.290	0.05
Electrical Installations	0.580	0.10
Thermal Insulations	0.464	0.08
Total	9.47	

In addition to direct costs, the indirect costs shown in Table 6 include engineering and design, plant construction, legal and contractors fees, and project contingencies.

Table 6. Indirect costs for the CHHP system.

	Cost (M€)	Factor (% DC)
Engineering and Design	1.42	0.15
Site prep and construction	1.42	0.15
Project contingency[1]	1.23	0.10
Total	4.07	

In this manner, the total investment respecting the CHHP system established is 13.54 M€. This value is higher than the one determined in [27] which is approximately 4.66 M€. The main factor for this discrepancy is related to the SOFC system cost, which in [27] is 0.850 M€ in comparison with 4.001 M€ provided by Bloom Energy. Nevertheless, the referenced value in [27] is obtained through the literature based on the US Department of Energy cost target for SOFC systems and not in the actual value of these systems in the market [36].

4.2 Consumption Costs and Production Profit

The consumption costs taken into consideration were related to fuel gas, water, and electrical energy. Considering the electrical energy consumption of the main equipment in the CHHP system, a total of 463.5 kW was determined. The amount of electrical energy available for the cogeneration system is only 603 kW, far inferior to the one expected to deliver. Considering 15.23 mol/h of fuel, 10 kmol/h of water and 357.1 kmol/h of air the total of energy produced by the SOFC is 1.744 MW.
A total consumption of 715 kW was reached, meaning 1.03 MW of electrical energy is available for GTs auxiliary equipment, as intended. A total investment of 20.045 M€ was determined.

Before studying the profitability with the data provided along with this chapter, there is one crucial aspect that should

also be analyzed in further detail, which is related to CO_2 emissions. These emissions remain the main factor in greenhouse gases, and their increase occurs mainly due to the harmful use of polluting (non-renewable) energies. Consequently, taxes on carbon emissions are imposed in most countries in order to mitigate pollutant emissions [37]. Nowadays, these have reached around 50 € ton^{-1} of CO_2 emitted. Nevertheless, this value is increasing substantially in the past months, and the tendency is to continue. Ideally, a SOFC only produces water if fuelled with pure hydrogen, since in this case, there are other components in the fuel, CO_2 will be produced. Yet, these emissions are still lower (0.308 kg/kWh) than the ones produced in a conventional electric power facility (0.429 kg kWh^{-1}) [38, 39]. Hence, the amount of capital saved using this system to produce electrical energy was considered a profit and will be included in the revenue obtained from the amount of electricity, hydrogen, and heat produced.

Table 7. CO_2 emissions and savings for the 1.744 MW CHHP system.

	SOFC	Power Plant	Units
CO_2 emissions	0.308	0.429	kg kWh^{-1}
Power	1 744		kWh
CO_2 emissions	0.538	0.748	ton/h
CO_2 emissions	4 297	5 979	ton $year^{-1}$
Carbon tax	50.0		€/ton
Total fare	214 831	298 971	€
Savings	84 140		€

Afterward, to analyse the economic performance associated with the project under evaluation, the Payback was calculated.

4.3 Investment Performance Indicator – Payback

Payback, defined as the time required for a project to recover the capital invested, is a measure of project risk.

Ideally, this indicator ought to be less than 5 years due to the SOFCs lifetime. For the proposed scenario, the Payback is 8 years which is far from being suitable. For this reason, increasing the profit, whether from an increase in the electrical energy produced or hydrogen, was tested. It was observed that this last one had a more significant impact in reducing the Payback in comparison with the electrical energy production, mainly due to the difference in the price set for both (the price for pure hydrogen is 120 times higher than the one considered for electrical energy). Thus, from an economic point of view, favoring a scenario that values the hydrogen over production is much more profitable, despite causing an increase in the auto-consumption of the equipment and consequently a reduction in the electrical energy distributed. Considering 22.5 kmol h-1of fuel gas, 19.5 kmol h-1of water and 357.1 kmol h-1air and setting the price for hydrogen on 15€/kg allows a Payback of 3 years and 2 months with yearly revenue of 8.496 M€. Although in the years where the SOFC system is replaced this value drops, it is still positive and corresponds to 1.404 M€.

5. Conclusions

The CHHP system was developed in Aspen Plus V11 software in order to determine its feasibility. Two different SOFC models were tested to calculate the cell voltage. Results indicate that to assure a reasonable hydrogen over production, with 219.8 kmol/h of air and 10 kmol/h of fuel gas, a cell voltage of 0.812 V is reached. Allowing for a power output of 1.067 MW and also delivering also 3.03 MMBtu/h of heat and 16.5 kg/h of hydrogen. An economic analysis was performed where the input conditions were corrected since the auto consumption of the main equipment in the system was considered. This resulted in a power production from the SOFC system of 1.744 MW, in order to deliver 1.03 MW to the GT auxiliary equipment. Additionally, the total investment, consumption costs and production profit were determined as well as the payback time. The total investment was 20.045 M€ and the payback time 8 years. Since this indicator should be below 5 years, the lifetime of the SOFC system, the impact of increasing the electrical energy and hydrogen produced was tested separately. Due to the difference between the hydrogen and electrical energy price, it has been concluded that favoring the hydrogen over production enables its reduction to 3 years and 2 months considering 22.5 kmol/h of fuel gas, 357 kmol/h of air and establishing the hydrogen price to 15€/kg. For this scenario, the hydrogen production reaches 70.1 kg/h (1 682 kg per day) and the electrical energy available for the cogeneration system is 677 kW.

References

[1] Xiongwen Zhang, S.H. Chan, Guojun Li, H.K. Ho, Jun Li, and Zhenping Feng. A review of integration strategies for solid oxide fuel cells. *Journal of Power Sources*, 195(3):685–702, 2010.

[2] Trevor Morgan. The hydrogen economy: A non-technical review. *United Nations Environment Programme*, 2006.

[3] Michael Reisert, Ashish Aphale, and Prabhakar Singh. Solid oxide electrochemical systems: Material degradation processes and novel mitigation approaches. *Materials*, 11(11):2169, 2018.

[4] Omar Z Sharaf and Mehmet F Orhan. An overview of fuel cell technology: Fundamentals and applications. *Renewable and Sustainable Energy Reviews*, 32:810–853, 2014.

[5] Brian Cook. Introduction to fuel cells and hydrogen technology. *Engineering science and education journal*, 11(6):205–216, 2002.

[6] Abdalla M Abdalla, Shahzad Hossain, Pg MohdIskandr Petra, Mostafa Ghasemi, and Abul K Azad. Achievements and trends of solid oxide fuel cells in clean energy field: a perspective review. *Frontiers in Energy*, 14(2):359–382, 2020.

[7] Prathak Jienkulsawad, Dang Saebea, Yaneeporn Patcharavorachot, Soorathep Kheawhom, and Amornchai Arpornwichanop. Analysis of a solid oxide fuel cell and a molten carbonate fuel cell integrated system with different configurations. *International Journal of Hydrogen Energy*, 43(2):932–942, 2018.

[8] R Mark Ormerod. Solid oxide fuel cells. *Chemical Society Reviews*, 32(1):17–28, 2003.

[9] Subhash C Singhal. Advances in solid oxide fuel cell technology. *Solid state ionics*, 135(1-4):305–313, 2000.

[10] J Will, A Mitterdorfer, C Kleinlogel, D Perednis, and LJ Gauckler. Fabrication of thin electrolytes for second-generation solid oxide fuel cells. *Solid State Ionics*, 131(1-2):79–96, 2000.

[11] M Sahibzada, BCH Steele, D Barth, RA Rudkin, and IS Metcalfe. Operation of solid oxide fuel cells at reduced temperatures. *Fuel*, 78(6):639–643, 1999.

[12] K Tanaka, C Wen, and K Yamada. Design and evaluation of combined cycle system with solid oxide fuel cell and gas turbine. *Fuel*, 79(12):1493–1507, 2000.

[13] The Green Growth Commitment and The Green Taxation Reform. https://www.crescimentoverde.gov.pt/wp-content/uploads/2014/10/2014_12_05_Portugal-\green-taxation-reforma-and-green-\growth-deal.pdf, 2014. [Online; Accessed 29-July-2021].

[14] Galp joins the Hydrogen Council and mulls projects to promote hydrogen economy in Portugal. https://www.galp.com/corp/en/media/press-releases/press-release/id/1043/\galp-joins-the-hydrogen-council-and-\mulls-projects-to-promote-hydrogen-\economy-in-portugal. [Online; Accessed 24-July-2021].

[15] Galp. *Manual Descritivo da Fábrica de Utilidades (internal information)*.

[16] M. Andersson and J. Froitzheim. Technology review - solid oxide cells, 2019.

[17] Jacob Brouwer, Ali Azizi, et al. Thermodynamic and dynamic assessment of solid oxide fuel cell hybrid systems for use in locomotives. Technical report, United States. Department of Transportation. Federal Railroad Administration, 2019.

[18] Bloom Energy Server ES5-250 kW. https://www.bloomenergy.com/resource/bloom-energy-server-es5-250kw/. [Online; Accessed 2-August-2021].

[19] Shaishav R Pandya, Vatsal M Shah, and Soham D Shah. Green manufacturing of electricity using sofc based bloom energy server tm.

[20] Mohd Kamaruddin Abd Hamid. Hysys®: An introduction to chemical engineering simulation, 2007.

[21] Mehdi Mehrpooya, Milad Sadeghzadeh, Ali Rahimi, and Mohammadhosein Pouriman. Technical performance analysis of a combined cooling heating and power (cchp) system based on solid oxide fuel cell (sofc) technology–a building application. *Energy Conversion and Management*, 198:111767, 2019.

[22] D Steward, M Penev, G Saur, W Becker, and J Zuboy. Fuel cell power model version 2: Startup guide, system designs, and case studies. modeling electricity, heat, and hydrogen generation from fuel cell-based distributed energy systems. 2013.

[23] P Spath, Andy Aden, T Eggeman, Matthew Ringer, B Wallace, and J Jechura. Biomass to hydrogen production detailed design and economics utilizing the battelle columbus laboratory indirectly-heated gasifier. Technical report, National Renewable Energy Lab., Golden, CO (US), 2005.

[24] Inc EG&G Technical Services. Handbook, fuel cell. *US Department of Energy, Office of Fossil Energy, National Energy Technology Laboratory-Morgantown, West Virginia*, 2004.

[25] Stefano Campanari. Thermodynamic model and parametric analysis of a tubular sofc module. *Journal of Power Sources*, 92(1):26–34, 2001.

[26] Wayne Doherty, Anthony Reynolds, and David Kennedy. Modelling and simulation of a biomass gasification-solid oxide fuel cell combined heat and power plant using aspen plus. 2009.

[27] WL Becker, RJ Braun, M Penev, and M Melaina. Design and technoeconomic performance analysis of a 1 mw solid oxide fuel cell polygeneration system for combined production of heat, hydrogen, and power. *Journal of Power Sources*, 200:34–44, 2012.

[28] Roberto Bove, Piero Lunghi, and Nigel M Sammes. Sofc mathematic model for systems simulations. part one: from a micro-detailed to macro-black-box model. *International Journal of Hydrogen Energy*, 30(2):181–187, 2005.

[29] Paola Costamagna, Azra Selimovic, Marco Del Borghi, and Gerry Agnew. Electrochemical model of the integrated planar solid oxide fuel cell (ip-sofc). *Chemical Engineering Journal*, 102(1):61–69, 2004.

[30] Ryan O'hayre, Suk-Won Cha, Whitney Colella, and Fritz B Prinz. *Fuel cell fundamentals*. John Wiley & Sons, 2016.

[31] Pilar Lisbona, Alessandro Corradetti, Roberto Bove, and Piero Lunghi. Analysis of a solid oxide fuel cell system for combined heat and power applications under non-nominal conditions. *Electrochimica Acta*, 53(4):1920–1930, 2007.

[32] W Zhang, Eric Croiset, Peter Lewis Douglas, MW Fowler, and E Entchev. Simulation of a tubular solid oxide fuel cell stack using aspenplustm unit operation models. *Energy Conversion and Management*, 46(2):181–196, 2005.

[33] Katie Fehrenbacher. 10 things you should know about Bloom Energy's IPO. https://www.greenbiz.com/article/10-things-you-should-know-about\-bloom-energys-ipo, 2018. [Online; Accessed 15-August-2021].

[34] Julia Kagan. Payback Period. https://www.investopedia.com/terms/p/paybackperiod.asp, 2021. [Online; Accessed 17-August-2021].

[35] João Miranda Reis. Estimativa do Investimento e Avaliação Económico-Financeira do Projecto de uma Nova Fábrica, 2020.

[36] Kristin Gerdes, E Grol, D Keairns, and R Newby. Integrated gasification fuel cell performance and cost assessment. *National Energy Technology Laboratory, US Department of Energy*, pages 1–26, 2009.

[37] Assaad Ghazouani, Wanjun Xia, Mehdi Ben Jebli, and Umer Shahzad. Exploring the role of carbon taxation policies on co_2 emissions: Contextual evidence from tax implementation and non-implementation european countries. *Sustainability*, 12(20), 2020.

[38] CO2 Emissions per kWh of Electricity Generated in France. https://www.rte-france.com/en/eco2mix/co2-emissions, 2021. [Online; Accessed 18-August-2021].

[39] Product Datasheet: Energy Server 5, 2019.